International Journal of
INTELLIGENT SYSTEMS AND APPLICATIONS IN ENGINEERING
ISSN:2147-6799 www.ijisae.org Original Research Paper

A Study on the Optimization of Process Parameters and their Effects on the Mechanical Properties of the Magnetic Pulse Welded AA 6061 T6 Tubular Joints

Pravin Kumar M.[1], Varahamoorthi R.[2], Sundarraj C.[3]

Submitted: 04/05/2024 **Revised**: 17/06/2024 **Accepted**: 25/06/2024

Abstract: Judicious selection of materials for light weight structures require high strength-to-weight ratio and good corrosion resistance alloys. AA 6061 alloy with such properties has attracted the attention of researchers around the globe. Joining of Aluminum using conventional fusion welding methods has been a challenge owing to its properties like ductility, high thermal conductivity and high reflectivity. Magnetic Pulse Welding (MPW) is a modern day state of the art "cold welding" process or more precisely a "solid state welding" process that can produce clean and precise joints of Aluminium alloys. MPW uses electromagnetic forces to weld two similar or dissimilar materials through high-speed impact of the metals due to a controlled acceleration. In this investigation, an attempt is made to optimize the significant process parameters of MPW for obtaining maximum Tensile strength of the AA 6061 T6 tubular joints. The joint strength of MPW joints is highly dependent on the process parameters like Discharge Voltage, Standoff distance and Overlap length and hence these parameters are considered for analysis and optimization. Design of Experiment (DOE) statistical tool was adopted for the systematic conduct of the tests. Response Surface Methodology (RSM) was embraced to develop the empirical relationship. AA 6061 T6 MPW joints were produced in lap configuration using a 100kJ capacity B-Max made MPW equipment. The welded specimens were prepared for tensile testing using Wire cut EDM. A maximum tensile strength of 303 MPa was observed for the parameter values of Discharge Voltage 12kV, Stand-off Distance 1.75mm and Overlap length of 8mm. The maximum tensile strength obtained is 98.05% of the actual Tensile Strength of the base metal. The Tensile Strength predicted through RSM was 303.04 MPa which is almost equal to the experimental value. The Contour and three-dimensional surface plots showing the interaction effect of the influencing process parameters on the tensile strength were developed. It was found that the Discharge Voltage and Stand -off distance affect the strength of the joint largely as compared with the Overlap length. Microhardness survey was conducted across the base metal and the weld interface and the results revealed that the Vicker microhardness was 138 HV at the weld interface and it varied from 108 HV to 120HV at the base metals. Microstructural study showed well defined wavy weld interface which is a personification of typical MPW joint. The results of the proposed model were validated using confirmation tests.

Keywords: *Magnetic Pulse Welding(MPW), AA 6061 T6, Design of Experiments (DOE), Response Surface Methodology(RSM), Tensile shear strength, Microhardness*

1. Introduction

Magnetic pulse welding (MPW) is a high-speed, solid state welding process that has the potential to significantly reduce manufacturing costs, especially for joining tubular structures. As a result of the increasing use of tubular components in current and future car designs, automotive engineers are looking to develop high-productivity, low-cost, and robust joining processes for tube connections. The trend of incorporating hydro formed tubular components and aluminium alloys into vehicle designs makes this process a prime candidate for high production automotive welding. In addition, the opportunity to join dissimilar materials (in particular, steel to aluminium) makes this process very attractive for car manufacturers [1]. MPW technology is applicable to tube-to-tube or tube to-bar configurations. Parts are configured to form a nominally lap-type joint. The process essentially functions by discharge of charged capacitors into an induction coil that encompasses the parts to be joined [2, 3].

The basic minimum necessary equipment for MPW process are a high power source, the capacitor, a discharge switch and a coil [Fig. 1]. The process works on Lenz law according to which a high intensity current near an electrically conductive material flowing through a coil, produces locally an intense magnetic field generating eddy currents in the flyer. Due to this induced electromotive force current is produced whose magnetic field opposes the original change in magnetic flux. This results in the generation of a Lorentz force, which accelerates the flyer at a very high speed. Upon placing a metal in the trajectory of the flyer, an atomic bond is produced by the impact of high velocity flyer resulting in a solid state weld.

[1]*Research Scholar, Annamalai University, Department of Manufacturing Engineering, Faculty of Engineering and Technology, Annamalai University, Chidambaram- 608002, Tamilnadu, India. Email: pravin@pkiet.edu.in.*
[2]*Professor, Annamalai University, Department of Manufacturing Engineering, Annamalai University, Chidambaram- 608002, India.*
[3]*Professor/Principal, AVC College of Engineering, Mannampandal, Mayiladuthurai, Tamilnadu, India.*

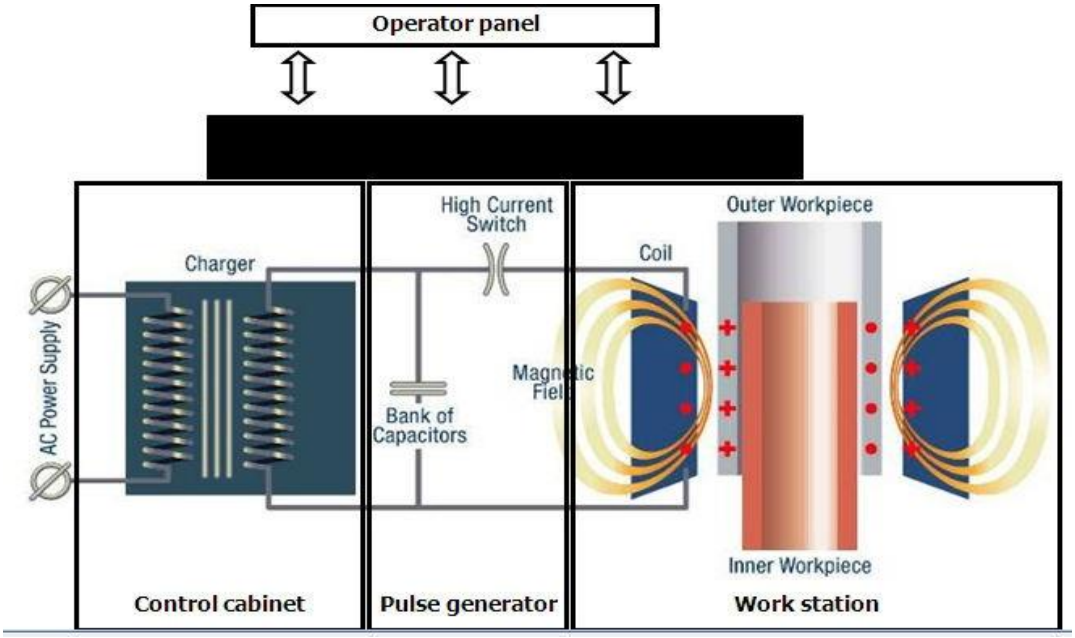

Fig. 1. Layout of MPW Process for Producing Tubular Joints

Though Magnetic pulse welding technique is known for a long time, it has not found a significant place amongst mainstream manufacturing processes and there are still opportunities of development and application, especially for joining multi-materials [4]. The possibility of joining dissimilar materials keeping intact their mechanical and chemical properties is seen as one of the main advantages of MPW as there is no heat introduced and no thermal distortions during joining. Due to the formation of jet during the high velocity impact between both materials, any oxidation and dirt in the materials are conveniently removed from the surfaces. Hence, MPW is considered to be a clean process where (Fig.2) [4] that do not emit harmful fumes or radiation.

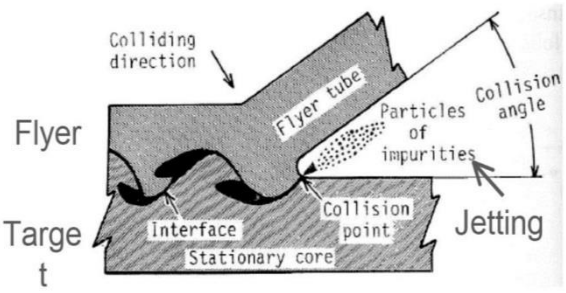

Fig. 2. Scheme of impurity removal, Jetting

Aluminium alloys, being light in weight, are best suitable for application in aerospace, nuclear, shipbuilding, railway, appliances and automobile industries. For improved fuel economy and reduced CO2 vehicle emission for environmental benefits, low-cost and light-weight materials are gaining demand in major automobile industries. Aluminium 6061 finds its wide application in aircraft and aerospace industries, in marine fittings, in camera lenses, electrical fittings, automotive parts and alike. aluminium possesses high thermal conductivity, high thermal expansion coefficient, low melting temperature making it's welding different than others. Also, the advantage of MPW technique over traditional welding techniques is that a tubular weld joint can be produced in less than a second and in welding aluminium, it does not produce the heat-affected zone and/or other weld defects, which are typical of conventional fusion welding processes. Moreover, for heat treated aluminum alloys, joints of very good quality can be produced with this technique. This welding technique is presently used in limited application such as sheet to sheet but welding of tube to flange is not yet studied widely and reported [5]. In this study, an attempt has been made to study the MPW joints of Al 6061tube to rod in lap configuration.

2. Magnetic Pulse Welding System

Welding experiments were conducted using a B-Max made MPW equipment [Fig 3]. Welding was performed by electromagnetic compression. The maximum energy of the system was 100kJ, maximum discharge 25kV and Maximum Discharge frequency was 60kHz. Capacitor bank of 160 µF and Single turn coil of diameter 68 mm and thickness 30mm were used for the study [Fig. 4]. High density Polyethylene (HDPE) fixtures and stoppers were used for precise positioning of the workpiece [Fig.5 and Fig. 6]. Single pulse was used for producing the joints.

Fig. 3. MPW Equipment

Fig. 4. Single Turn Coil

Fig. 5. HDPE Fixture

Fig. 6. Coil with Stopper

3. Experimental Procedure

3.1 Material

Al 6061 T6 was chosen as the workpiece material with Flyer metal in Tube form and the Target metal in rod form [Fig. 8 & 9]. The chemical composition of Al 6061 T6 and their mechanical properties are furnished in Table 1 and Table 2.

Table 1. Chemical Composition of Al6061 T6

% Si	% Mg	%Mn	%Fe	% Cr	% Cu	% Zn	% Ti	% V	% Zr	% Al
0.0740	0.850	0.040	0.130	0.090	0.250	0.010	0.020	0.003	0.003	0.9757

Table 2. Mechanical Properties of Al6061 T6

Tensile strength (MPa)	Yield Strength (MPa)	% Elongation	Fatigue Strength (MPa) at 500 mil cycles	Melting Point (ºC)	Thermal Conductivity (W/mk)	Density (kg/m^3)	Youngs Modulus (GPa)	Hardness (Vickers)	Electrical Resistivity (ohm-m)	Permeab-ility (µ)
309	276	10	97	650	209	2.7x10^3	70	80	4.32e-8	1

3.2 Significant Process parameters:

From the excerpts of literatures [6], [7], [8], [9] and [10], significant process parameters of MPW were selected as Discharge Voltage(V), Stand- off Distance (d) and the Overlap length(L) for this work.

- **Discharge Voltage (V)**

The energy that is stored in the capacitor bank is responsible for the movement of the flyer metal as it gets discharged into the coil. In order to accelerate the flyer metal at high velocity to create huge impact, energy is discharged in a very short span of time in the range of a few microseconds.

The shearing strength of the welds is improved upon increase in the charging voltage or the capacitance of condensers or increase in the discharge energy [4]. For producing the joint, there is a threshold value of the discharge voltage and utmost care must be taken while choosing correct range of energy to avoid exceeding critical strain rate of the material that can tear them.

- **Stand -off Distance (D)**

It is the distance between parts to be joined before the discharge of energy [Fig 7]. When magnetic pressure is applied on the flyer metal this gap must have sufficient space to gain velocity and acquire kinetic energy that can be transformed into impact energy. Like Discharge Voltage. An optimum value of standoff distance must be selected based on the welding materials to realize required joint strength.

- **Overlap Length (L)**

It is the length of the Flyer metal that is exposed to coil [Fig 7]. The overlap length is a material-dependent parameter that influences the impact angle.

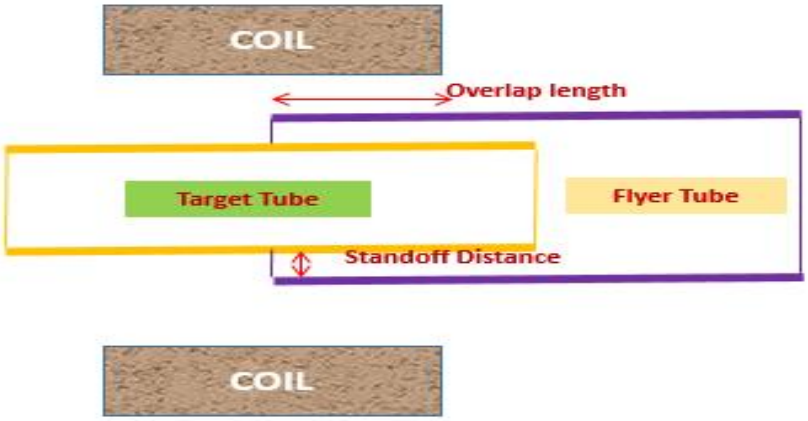

Fig. 7. Joint Configuration

3.3 Trial Experiments:

Trial experiments were conducted with the set of parameters as detailed in Table 3. Before welding, the bars and tubes were sanded with 320-grit papers, and then cleaned with acetone. For all the trials, the end of the tubes was even with the edge of the concentrator. The bars were inserted into the tubes to obtain the desired overlap length as illustrated in [Fig 11 & 12].

Table 3. Trail Experiment Parameter details

Parameters	Trail 1	Trail 2	Trail 3	Trail 4	Trail 5
Discharge Voltage(kV)	12	14	16	18	20
Stand-off Distance(mm)	1.75	2	2.25	2.5	2.75
Overlap length (mm)	7	7.5	8	8.5	9

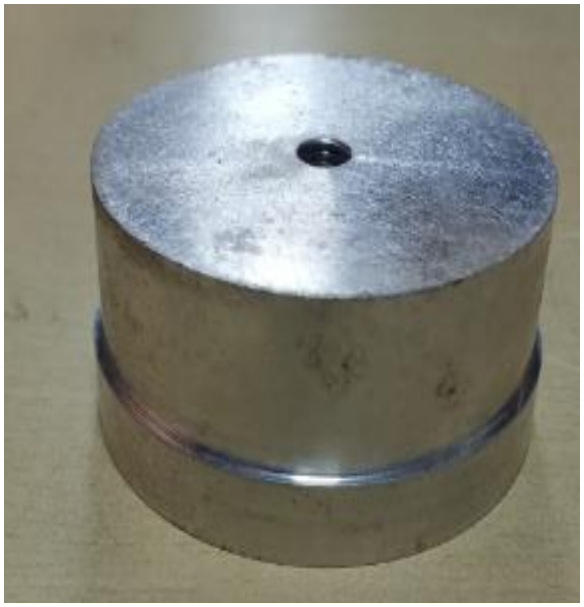

Fig. 8. Al6061 T6-Target (Before weld)

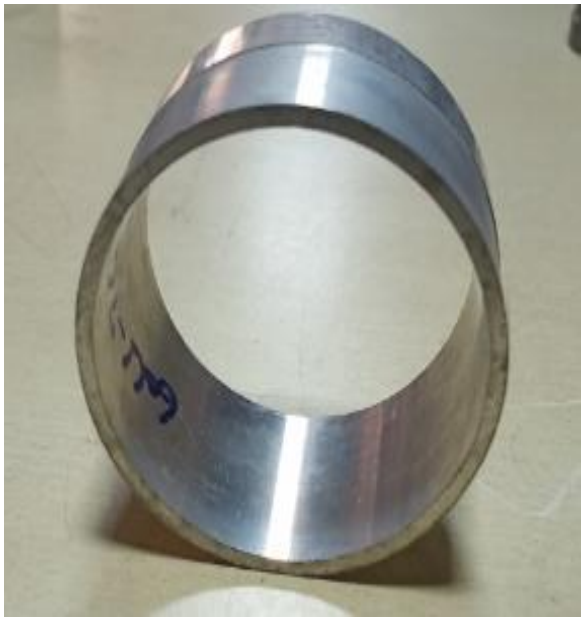

Fig. 9. Al6061 T6-Flyer (Before weld)

Fig. 10. Flyer-Target After Weld

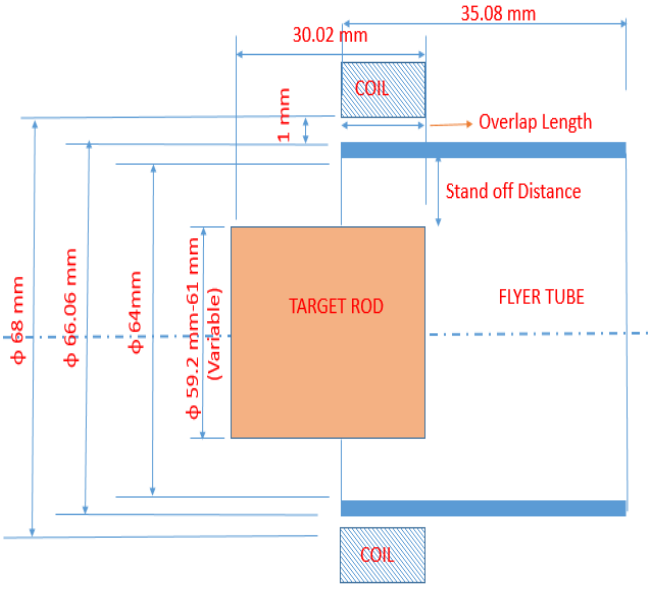

Fig. 11. Flyer-Target Dimensions

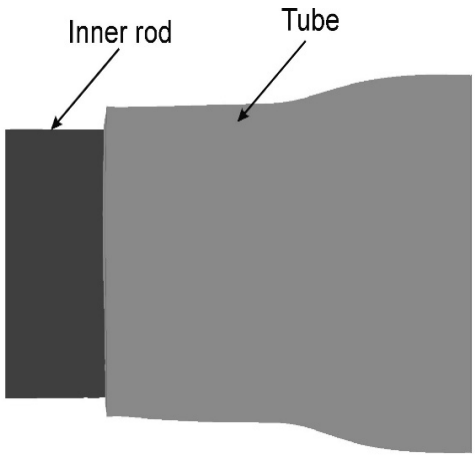

Fig. 12. MPW Specimen -Schematic

Manual Peel tests were conducted for qualification of the weld result as shown in Fig. 8. The flyer metals were cut axially into Strips of width 20mm approximately and bent radially [10]. If the flyer part failed in the base material during peel test, the strength of weld seam was considered sound.

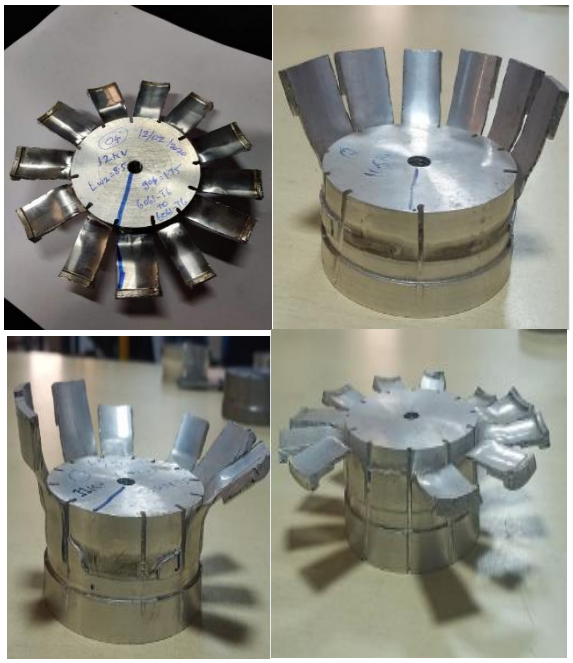

Fig. 13. Peel tested specimen

3.4 Design of Experiments:

Based on the results of peel tests, the range of process parameters were selected as Discharge Voltage (V) – 12 kV to 16 kV, Stand-off distance (D) – 1.75mm to 2.5mm and Overlap lap length (L)-7.5mm- 8mm. Experiments were conducted as per the design matrix [Table 5] employing Central Composite Design (CCD) using Design Expert Version 11 software. The specimen dimensions of the target metal rod 200mm length, 63 mm diameter whereas for the Flyer tube 200mm length, 68 mm diameter. 25mm length of the flyer was drilled for an inner diameter of 64mm and outer diameter of 66mm for a partly length of 25 mm. For the desired Stand-off distance, the diameter of the target rod was machined and for obtaining the desired Overlap length, the length of the work pieces exposed to the coil were adjusted.

Table 4. MPW Process Parameters and their levels

Parameters / levels	**-1.68**	**-1**	**0**	**+1**	**+1.68**
Discharge voltage (kV)	10.64	12	14	16	17.36
Stand- off distance (mm)	1.58	1.75	2	2.25	2.42
Overlap length (mm)	7.33	7.5	7.75	8	8.17

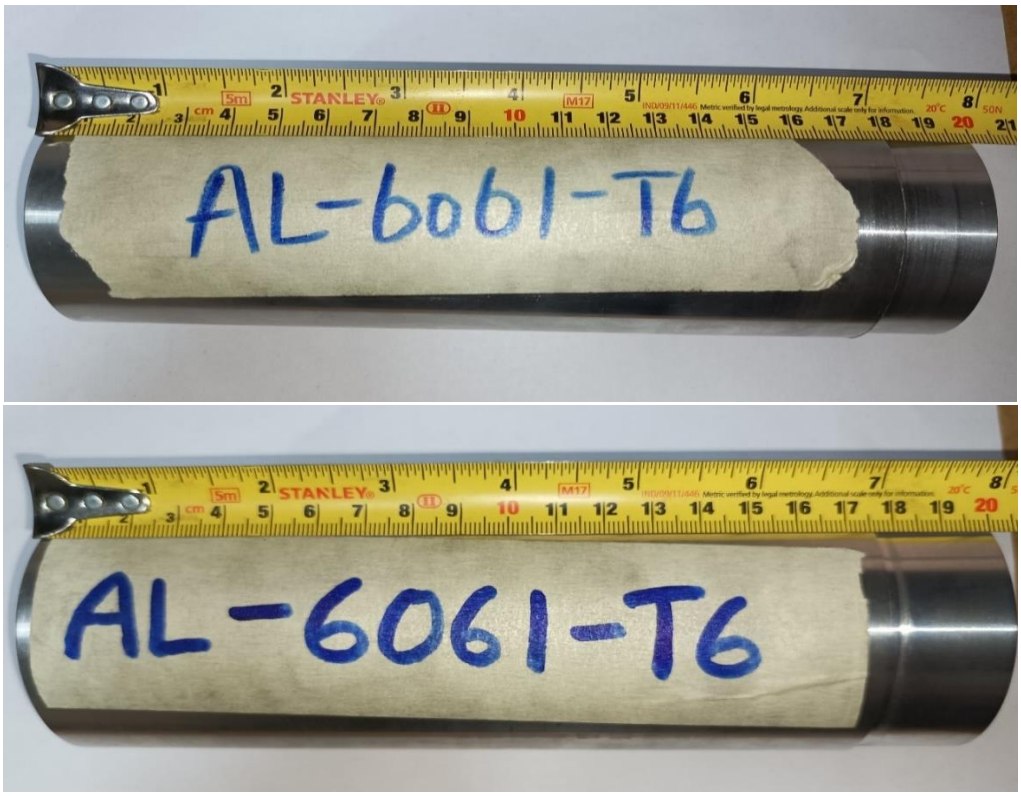

Fig. 14. Specimen before weld

20 nos. of experiments were conducted as per the Design Matrix
Table 5

Fig. 15. Specimen after weld

Fig. 16. Weld Specimen (20 nos.)

Table 5. Design Matrix with Coded and Actual values

EX. NO.	Coded Values			Actual Values		
	DV	SOD	OL	DV (kV)	SOD (mm)	OL (mm)
1	-1	-1	-1	12	1.75	7.5
2	+1	-1	-1	16	1.75	7.5
3	-1	+1	-1	12	2.25	7.5
4	+1	+1	-1	16	2.25	7.5
5	-1	-1	+1	12	1.75	8
6	+1	-1	+1	16	1.75	8
7	-1	+1	+1	12	2.25	8
8	+1	+1	+1	16	2.25	8
9	-1.68	0	0	10.64	2	7.75
10	+1.68	0	0	17.36	2	7.75
11	0	-1.68	0	14	1.58	7.75
12	0	+1.68	0	14	2.42	7.75
13	0	0	-1.68	14	2	7.33
14	0	0	+1.68	14	2	8.17
15	0	0	0	14	2	7.75
16	0	0	0	14	2	7.75
17	0	0	0	14	2	7.75
18	0	0	0	14	2	7.75
19	0	0	0	14	2	7.75
20	0	0	0	14	2	7.75

4. Tensile Testing

Tensile Strength testing was carried out using 1000 N capacity Tinius Olsen model Universal Testing machine as shown in Fig 21. It has a speed resolution of about 0.001mm/min and a displacement resolution about 0.0001 mm. The tensile Specimen were prepared by slicing the MPW joints using Electric Discharge Machining (EDM) as shown in the [Fig.17,18,19 and 20] Two slices (samples) were prepared from each specimen.

Two samples were used to evaluate Tensile strength using the Universal Tensile Testing machine. The average of the two was considered the tensile strength as recorded in the Table 5. Fig 22 shows that the fracture of all the tensile specimen occurred at the flyer metal which personifies sound weld joint. Fig. 27 shows Stress-Strain variations of Experiment No. 5 at UTS of 303 MPa and % Elongation 2.24%, the curve traced depicts fracture of a typical ductile material.

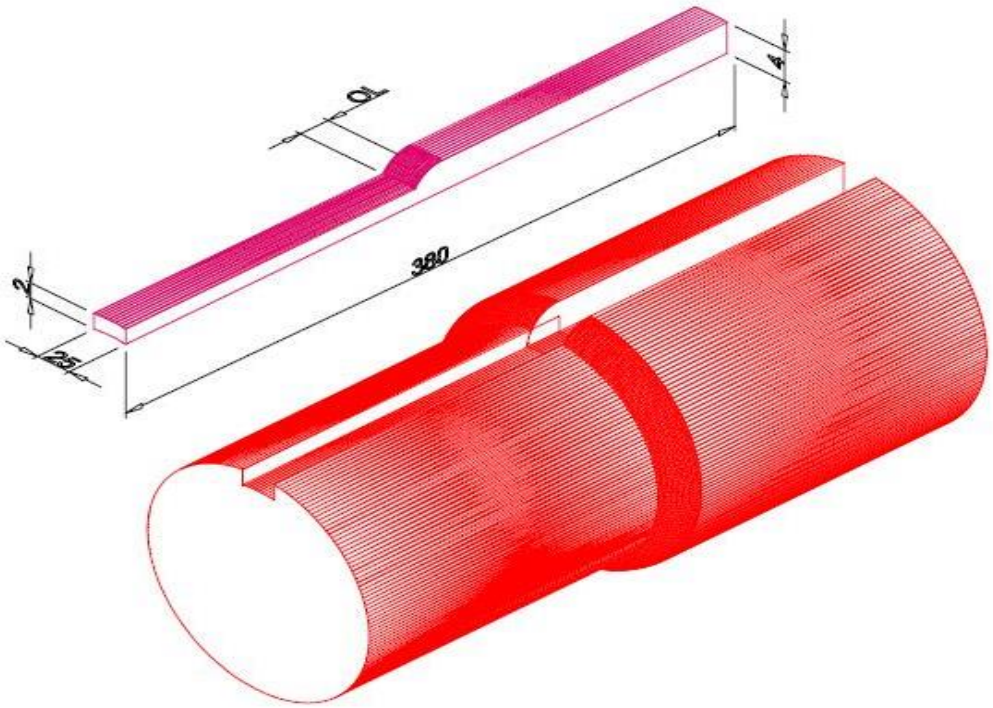

Fig. 17. Tensile Specimen

Fig. 18. Tensile Specimen

Fig. 19. Tensile Specimen- rear side

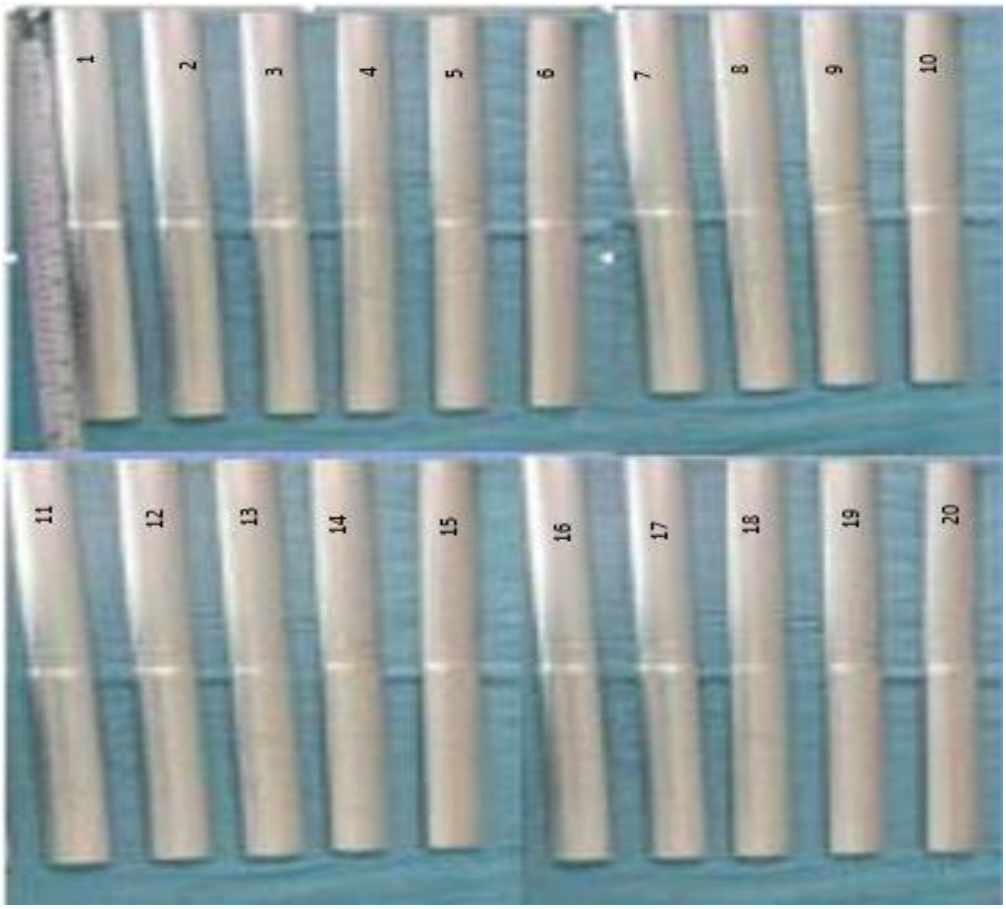

Fig. 20. Tensile Specimen Samples

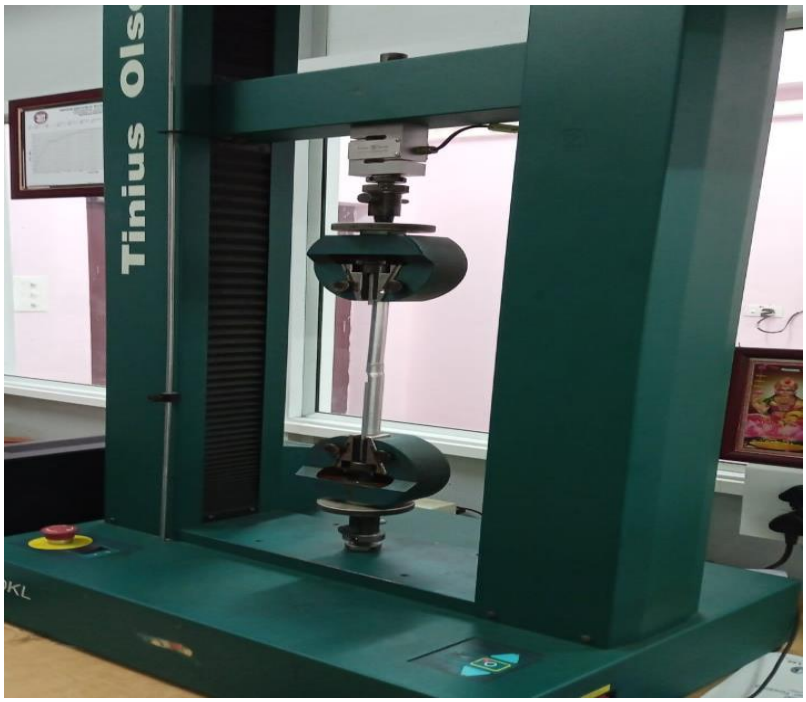

Fig. 21. UTM Equipment

Fig. 22. Specimen after Tensile Fracture

5. Development of Empirical Relationship

To predict the maximum Ultimate Tensile Strength (UTS) in terms of the MPW process parameters for AA 6061 T6 joints, a mathematical model was developed using Response Surface Methodology (RSM) technique. The response function of the joint (UTS) is a function of Discharge Voltage, Stand-off Distance and Overlap length.

UTS =f (DV, SD, OL)

The response "Y" is represented by the following general second order regression equation

$$\mathbf{Y = b_o + \Sigma\, b_i x_i + \Sigma\, b_{ii} x_i^2 + \Sigma\, b_{ij} x_i x_j + e_r}$$

The experimental results are fitted to the second order quadratic equation. From the CCD experiments, the predicted equation, including three factors is obtained as follows:

UTS = {(-3002.97699) + (94.46504 x DV) – (438.88968 x SD) + (812.51551 x OL) + (7.75000 x DV x SD) – (2.25000 x DV x OL) + (30.00000x SD x OL) – (3.76234x DV²) + (17.14655x SD²) - (53.71513x OL²)) **MPa**

ANOVA technique is used in this work to check the adequacy of the developed relationship. It is to be understood that the calculated F ratio value of the developed model must be less than the tabulated Standard F ratio at a desired confidence level (95%), if so the model can be considered to be adequate within the confidence limit.

Table 6 shows the ANOVA results and it can be understood that the developed model is adequate at 95% confidence level. The Model F-value of 557.29 implies the model is significant. There is only a 0.01% chance that an F-value this large could occur due to noise. P-values less than 0.0500 indicate model terms are significant. In this case DV, SD, OL, DV-SD, SD-OL, DV-OL, DV², SD², OL² are significant model terms. Values greater than 0.1000 indicate the model terms are not significant. If there are many insignificant model terms (not counting those required to support hierarchy), model reduction may improve this model.

The Lack of Fit F-value of 0.52 implies the Lack of Fit is not significant relative to the pure error. There is a 75.56% chance that a Lack of Fit F-value this large could occur due to noise. Non-significant lack of fit is good -- we want the model to fit.

6. Analysis of Variance (ANOVA)

Table 6. ANOVA Test Results

Source	Sum of Squares	DF	Mean Square	F Value	P value (Prob > F)	
Model	13331.62	9	1481.29	557.29	< 0.0001	Significant
A-DV	8967.52	1	8967.52	3373.77	< 0.0001	
B-SOD	732.29	1	732.29	275.50	0.0008	
C-OL	60.62	1	60.62	22.81	< 0.0001	
AB	120.12	1	120.12	45.19	0.0795	
AC	10.13	1	10.13	3.81	0.0087	
BC	28.12	1	28.12	10.58	< 0.0001	
A²	3253.54	1	3253.54	1224.05	0.0319	
B²	16.50	1	16.50	6.21	< 0.0001	
C²	161.91	1	161.91	60.91	< 0.0001	
Residual	26.58	10	2.66			
Lack of Fit	9.08	5	1.82	0.5189	0.7556	Not significant
Pure Error	17.50	5	3.50			
Cor Total	13358.20	19				

Fit statistics Table 7 shows that the Predicted R² of 0.9929 is in reasonable agreement with the Adjusted R² of 0.9962; i.e. the difference is less than 0.2. Adeq Precision measures the signal to noise ratio. A ratio greater than 4 is desirable. Your ratio of

92.298 indicates an adequate signal. This model can be used to navigate the design space.

Table 7. Fit Statistics

Standard Deviation	1.63	**R^2**	0.9980
Mean	269.70	**Adjusted R^2**	0.9962
C.V. %	0.6045	**Predicted R^2**	0.9929
		Adeq. Precision	92.2983

7. Optimization of MPW Parameters

The Criteria for numerical optimization as per the Table 8 and Fig 23 show the Goal, Limits Lower and Higher limit, Weight and Importance of each factor and response. The optimization tool used to search the optimum values of the parameters was Response Surface Methodology (RSM). Optimization was done with Coded values and then converted into actual values using Design Expert version 11 Statistical Software. The maximum Ultimate Tensile Strength obtained under optimized conditions was 303.04 MPa as shown in Table 9.

Table 8. Criteria For Numerical optimization

Parameter	Goal	Lower limit	Upper limit	Lower Weight	Upper Weight	Importance
A-Discharge Voltage	in range	12	16	1	1	3
B- Stand off Distance	in range	1.75	2.25	1	1	3
C- Overlap length	in range	7.5	8	1	1	3
Response- Ultimate Tensile Strength	maximize	197	303	1	1	3

Table 9. Optimized parameters

Condition	Discharge Voltage (kV)	Stand off Distance (mm)	Overlap length (mm)	Ultimate Tensile Strength (MPa)	Desirability
Experiment	12	1.75	8	303	---
Predicted by RSM	12.26	1.76	7.92	303.04	1

Fig. 24 clearly depicts Strong relationship between the Predicted and actual values of the response UTS. The results for R^2 value as shown in the normal probability plot for UTS reveal that the calculated and observed results within the range of experiment fall very close to each other. Table 15 illustrates the difference between the Experimental and Predicted values of the UTS. The perturbation plot Fig. 26 depicts how the response UTS changes when each factor Discharge voltage, Stand-off distance and Overlap length is increased or decreased. The percentage Error for each of the 20 experiments is less than 3% and hence, it is evident that there is very little difference between the Experimental and Predicted values for any particular set of process parameters.

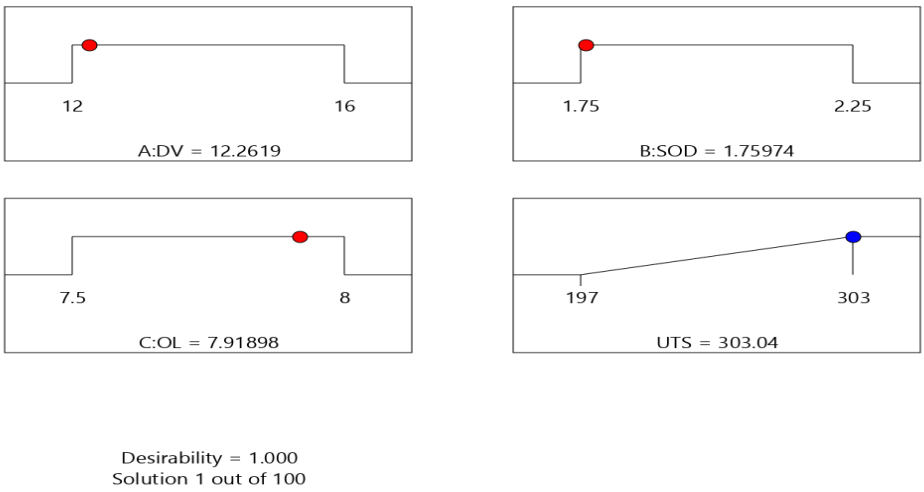

Fig. 23. Criteria of optimization

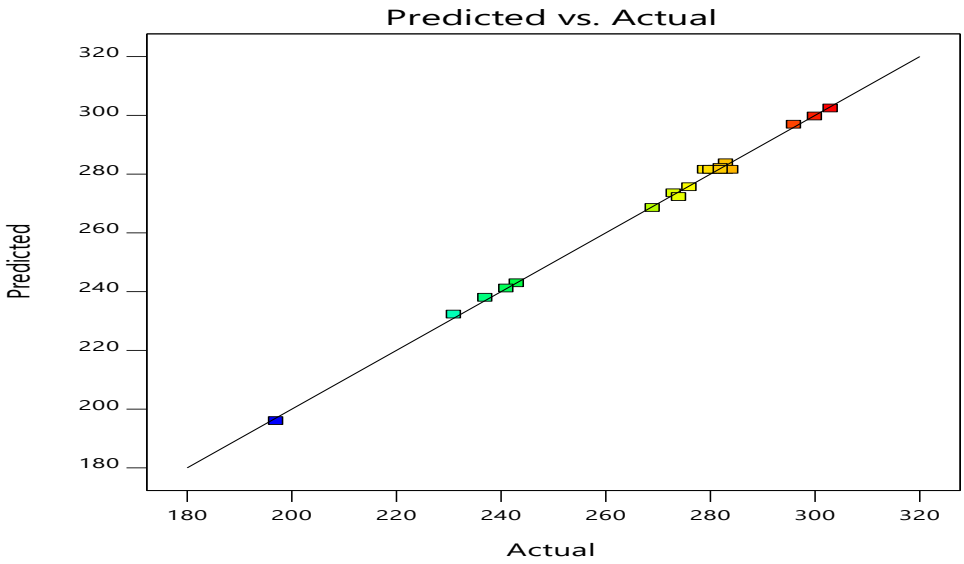

Fig. 24. Predicted vs Actual values

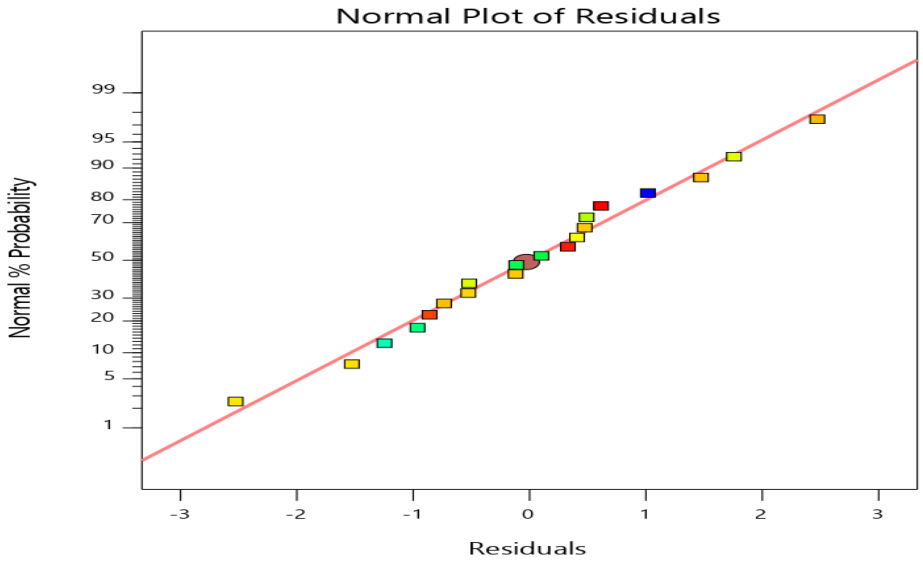

Fig. 25. Normal probability plot for UTS

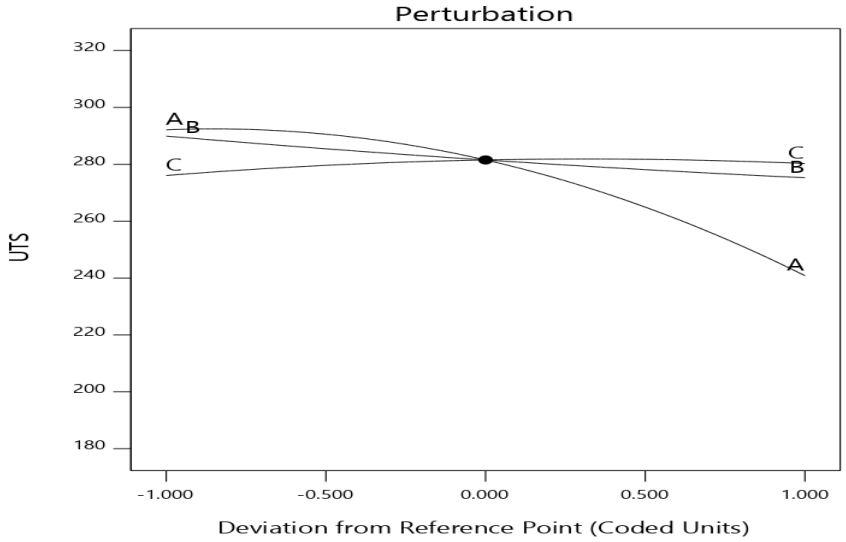

Fig. 26. Perturbation Plot

Table 10. Design matrix with Actual and Predicted UTS

EX. NO.	Actual Values			UTS (MPa) Experimental	UTS (MPa) Predicted by RSM	% Error
	DV (kV)	SOD (mm)	OL (mm)			
1	12	1.75	7.5	300	299.67	0.0033
2	16	1.75	7.5	243	242.90	0.001
3	12	2.25	7.5	273	273.52	-0.0052
4	16	2.25	7.5	231	232.25	-0.0125
5	12	1.75	8	303	303.04	-0.004
6	16	1.75	8	241	241.11	-0.0011
7	12	2.25	8	283	283.73	-0.0073
8	16	2.25	8	237	237.96	-0.0096
9	10.64	2	7.75	282	282.12	-0.0012
10	17.36	2	7.75	197	195.98	0.0102
11	14	1.58	7.75	296	296.86	-0.0086
12	14	2.42	7.75	274	272.24	0.016
13	14	2	7.33	269	268.51	0.0049
14	14	2	8.17	276	275.59	0.0041
15	14	2	7.75	281	281.53	-0.0053
16	14	2	7.75	283	281.53	0.0147

17	14	2	7.75	284	281.53	0.0247
18	14	2	7.75	279	281.53	-0.0253
19	14	2	7.75	280	281.53	-0.0153
20	14	2	7.75	282	281.53	0.0047

Width mm	Thickness mm	Area mm²	Ultimate Force N	Break Distance mm	Ultimate Stress MPa	Total Elongation (Auto) %
24.0	1.12	26.9	8150	6.27	303	2.24

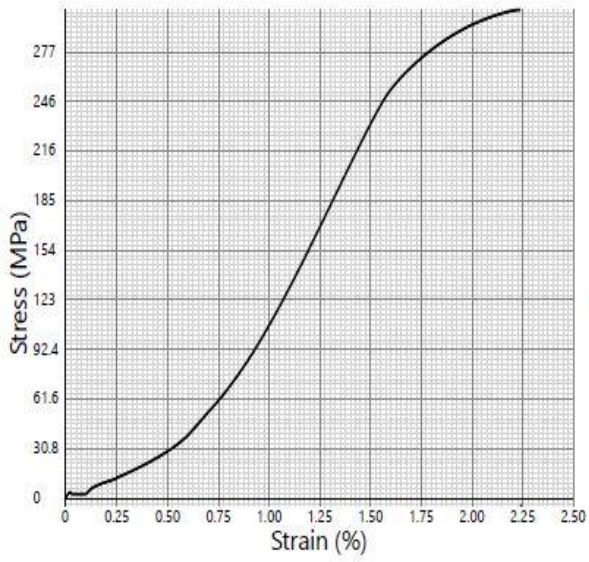

Fig. 27 (a). Stress –Strain Curve of Exp. No. 5

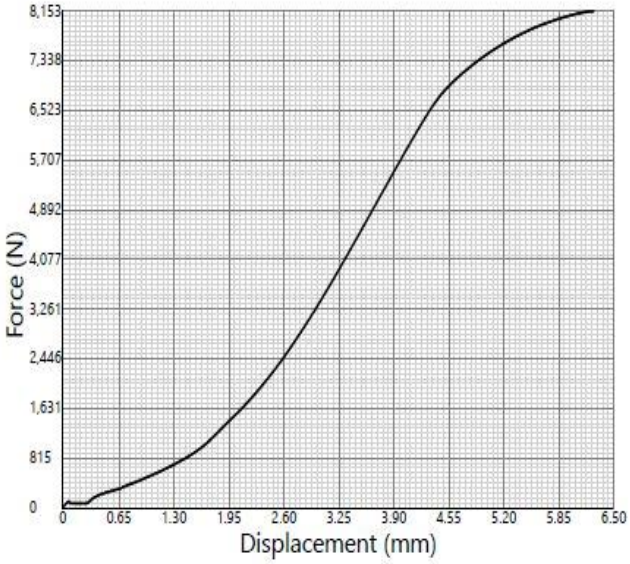

Fig. 27 (b). Force –Displacement Curve of Exp. No. 5

8. Contour Plots And Response Graphs

Response surfaces were developed for the empirical relationship, considering two parameters in the X and Y axes and the response in the Z direction. The response surfaces clearly indicate the optimal response point. The optimal Ultimate Tensile Strength (UTS) of the magnetic pulse welded AA 6061T6 tubular joint was observed at the apex of the contour response surface as shown in the figure. Contour plots generated for response surface analysis using Design expert software locates the optimum values with reasonable accuracy by characterizing the shape of the surface. Circular shape contour patterns indicate the independence of factor effects whereas elliptical contours indicate factor interactions.

The contour plot [Fig 28, 29 and 30] and 3D response plot [Fig 31,32 and 33] show the effect of parameters Discharge voltage and Stand-off distance on the response Ultimate tensile Strength. The plots clearly depict that the UTS is increasing initially when the Stand off distance increases from 1.5mm to 1.75mm and the same is showing decreasing trend if Stand off distance is increased beyond 1.75mm. Increase in voltage from 10kV to 13kV, there is increase in UTS and it decreases exponentially as the voltage is increased beyond 13 kV. For a Stand off distance of 1.75mm and Discharge Voltage 12 kV, maximum UTS of 303 MPa is reached and any increase in their values showed a decreasing trend of UTS. Increase in Stand off distance will enable the flyer tube take more time to reach the target and hence the required kinetic energy to cause severe plastic deformation of the metals may not be attained which leads to reduced tensile strength.

With increase in Overlap length at a given voltage, there is slight increase in UTS and a slight decreasing trend is observed afterwards as the Overlap length increases. Overlap length 7 to 7.75 mm shows increased UTS and UTS is seen decreasing because the area of the flyer at the open end is exposed to the coil in the middle which is subjected to high magnetic pressure. As per the Contour plot and 3D response plot , increase in Stand off distance at a given Overlap length, the UTS increases and shows mild decrease in its value.

Fig. 34 shows that there is tremendous decrease in UTS with increase of Discharge voltage beyond 13kV, Fig.35 shows that UTS decreases as the Stand off distance increases beyond 1.75mm. Fig 36 shows that UTS increases marginally for overlap length between 7 to 7.75mm and it decreases marginally beyond 7.75mm.

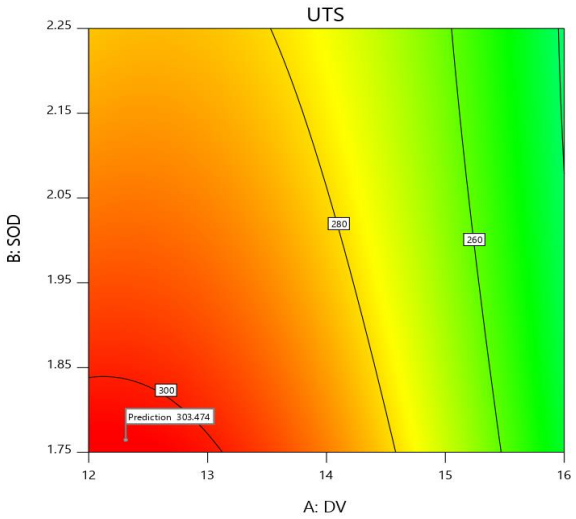

Fig. 28. Contour Plot - DV vs SOD

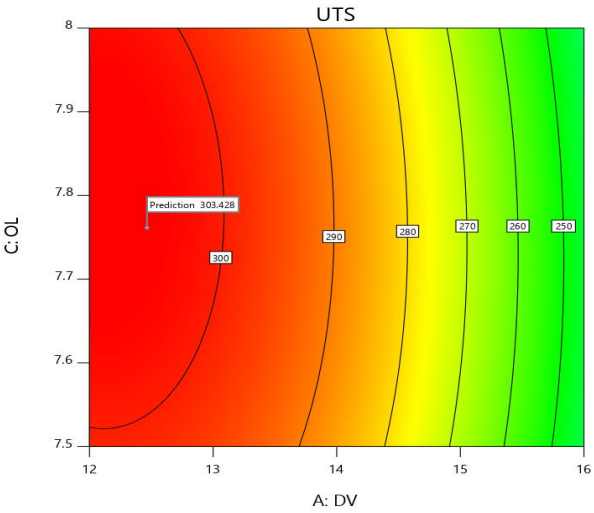

Fig. 30. Contour Plot- DV vs OL

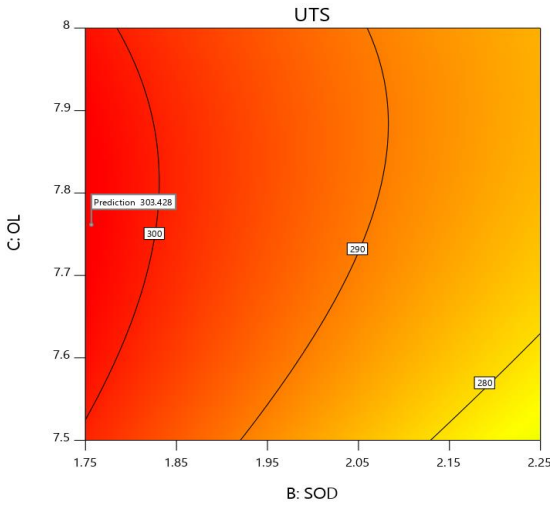

Fig. 29. Contour Plot- SOD vs OL

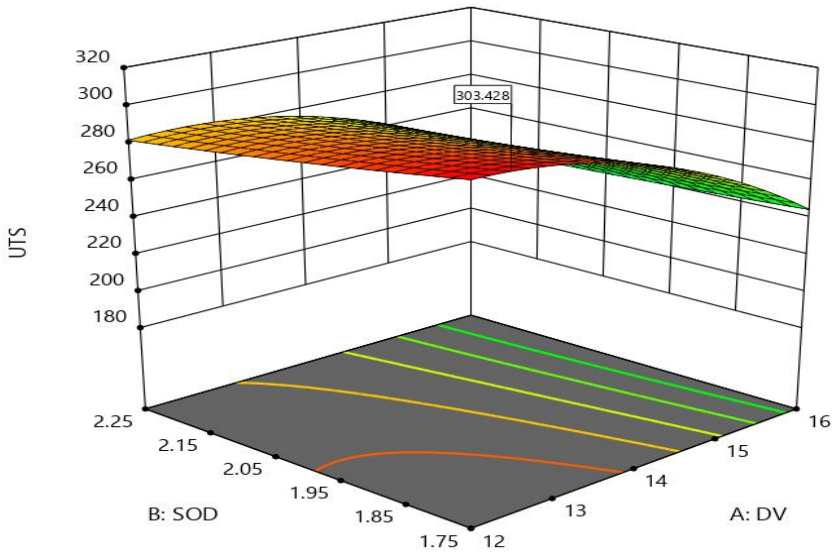

Fig. 31. 3D Response Graphs of UTS -DV vs SOD

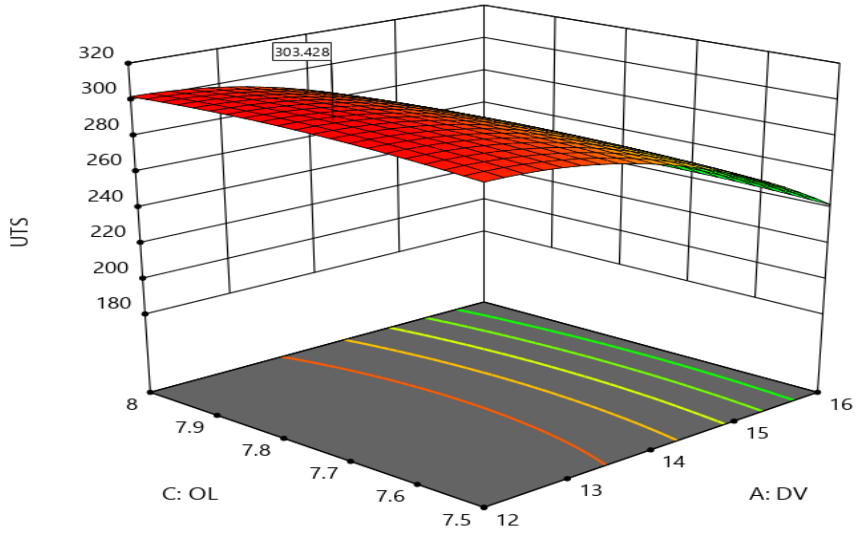

Fig. 32. 3D Response Graphs of UTS- DV vs OL

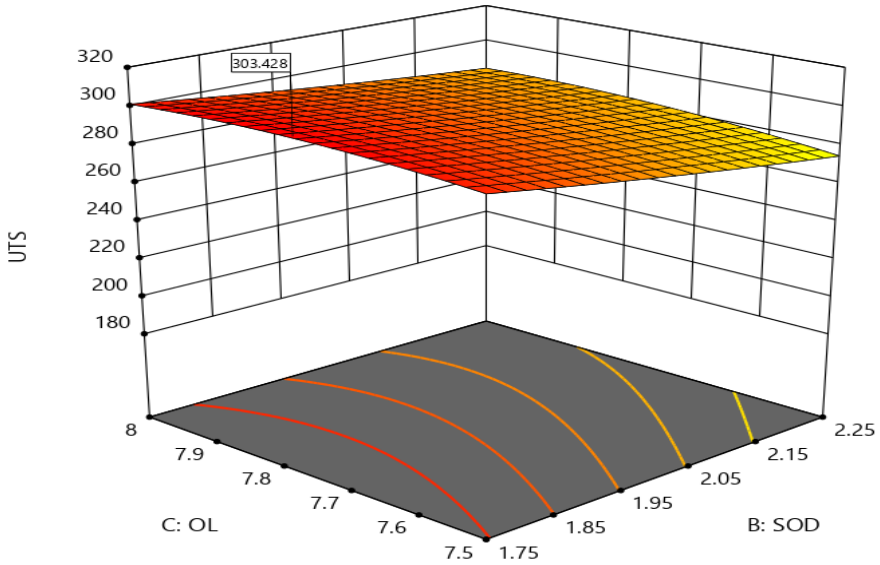

Fig. 33. 3D Response Graphs of UTS - SOD vs OL

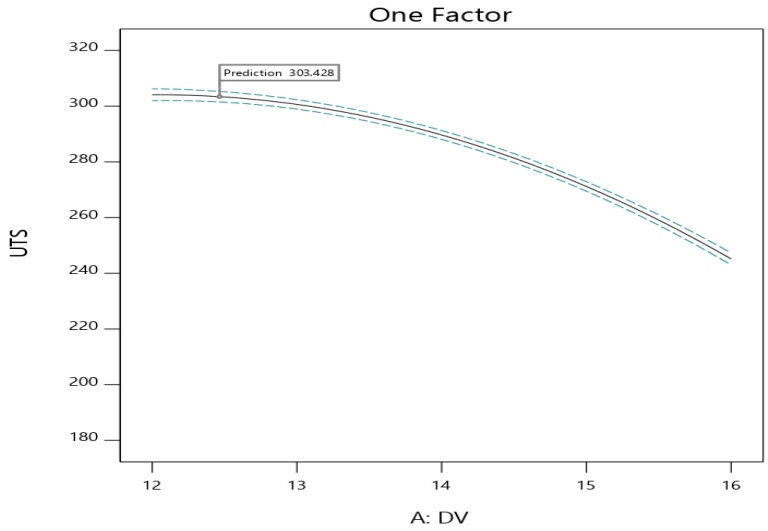

Fig. 34. Effect of DV on UTS

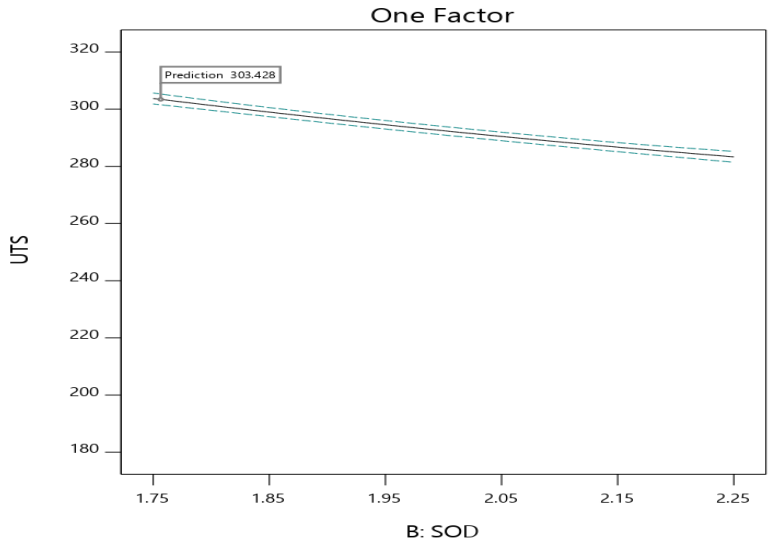

Fig. 35. Effect of Stand- off Distance on UTS

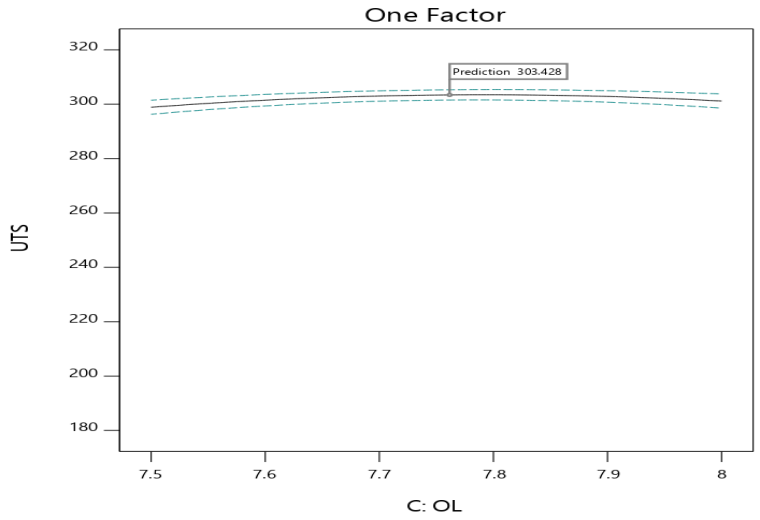

Fig. 36. Effect of Overlap Length on UTS

9. Validation of Optimized Procedure of UTS

Verification of the predicted UTS by RSM was done through conduct of five numbers of tests using the optimized parameters. The actual and predicted values are presented in the Table. It can be observed that the maximum percentage error is 3% between the actual and predicted values and hence the predictive optimisation technique method can be considered good.

Table 11. Validation of Optimized Procedure

Run Order	UTS (MPA)		
	Actual Value	**Predicted Value**	**% Error**
1	303	303.003	-0.03
2	283	283.997	0.003
3	197	197.002	-0.002
4	241	241.999	0.001
5	276	275.998	0.002

10. Microhardness Survey

Microhardness testing was done using Vicker's Microhardness testing machine, Metsuzawa, Japan MMT-X7/MMS250X make with range 5gm- 1kg. It was observed that the hardness value is higher in the weld zone 138 HV than the base metal target metal and Flyer which was falling between 108 HV to 117 HV as indicated in the Fig. 37.

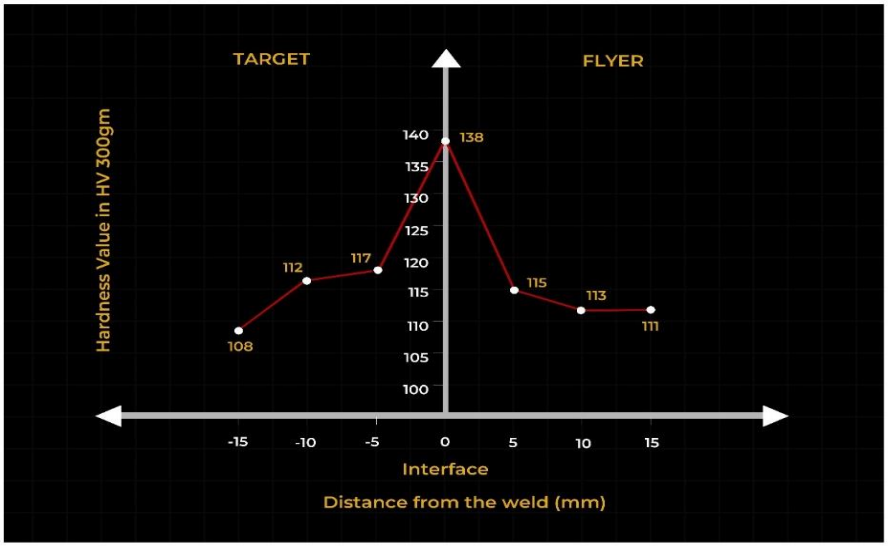

Fig. 37. Vicker's Microhardness Survey

The grains size refinement was possibly caused by rapid and Severe plastic deformation (SPD). The time for the flyer plate moving from stationary state to the peak velocity was regarded as the deformation process and the rapid deformation lasts for 10–20 μs. The plastic deformation induced heat could not dissipate quickly in this duration. There is a wavy nature of the welded interface and thus the local temperatures and the extents of deformation vary significantly from place to place. Pure adiabatic heating is modest. If strain levels are higher local adiabatic temperatures will rise accordingly. In many impact welds there is evidence of isolated local melting, but usually this is for a very small region of the weld interface. Since overall temperatures can be low in the transient impact welding process, little amount of recovery or recrystallization are expected. Thus the local work goes into structure refinement.

11. Microstructural Analysis

Microstructural studies using **FESEM** was done on the weld specimen at the weld interface, Target metal and the Flyer metal. Wire cutting machine was used to cut specimen along the center line of joints so as to avoid microstructural changes. To expose the center surface of joints, the samples were then embedded in phenolic. SiC abrasive paper was used to progressively ground all samples and then polished by a metal sample polishing machine. Finally, the metallographic samples were etched for 25 s by Keller's reagent (95 mL water, 2.5 mL HNO3, 1.5 mL HCL, 1.0 mL HF).

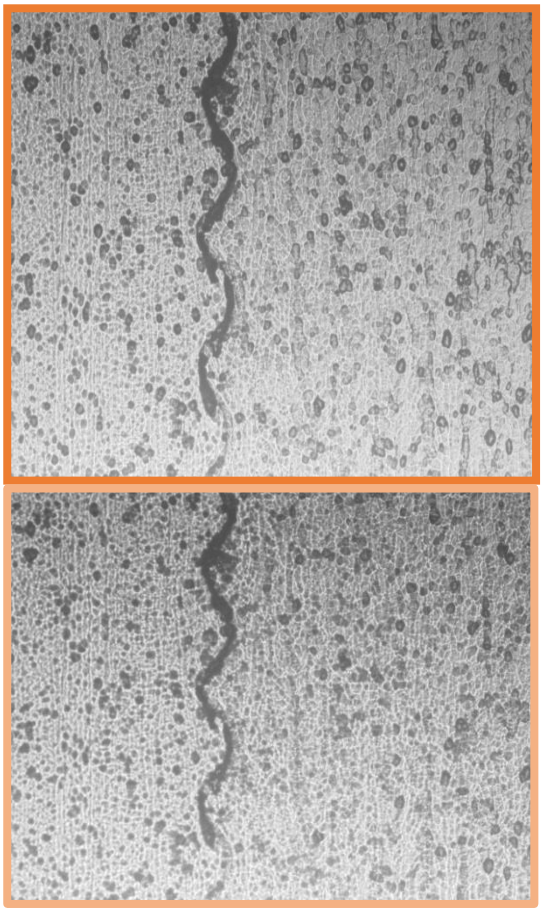

Fig. 38. SEM images of the weld sample having maximum UTS (100 μm)

A well-defined wave as shown in Fig.38 was formed in the weld interface area which is the personification of typical MPW joint. According to shock wave theory, Ben-Artzy et al [10] claims that shock waves propagate through the metal parts, creating periodic interference perturbation at the weld interface. These interferences initiate a Kelvin–Helmholtz instability that creates the interface waves. The initial gap influences the impact angle that sets the relationship between the collision point velocity and the weld propagation velocity. Also the energy of the capacitor and the initial gap determine the collision velocity of the outer

tube. The interface wavelength was found to be proportional to the geometry of the inner part. These are the main process parameters that influence interface wave formation. It was established that in tubular MPW joints, interface waves are formed in a Kelvin–Helmholtz instability mechanism, whereby reflected shock waves are the source for interferences at the weld interface. Interface waves are formed only at the impact zone and its vicinity, due to induced metal flow in this elevated temperature and high pressure region.

12. Conclusions

Magnetic pulse welding have been performed on Al 6061 T6 tube–rod in lap configuration successfully and the following conclusions were made.

1. The tensile shear strength for welded specimens have been determined. The Tensile testing was carried out as per the design matrix. The central composites design and the Response Surface Methodology (RSM) is used to develop the empirical relation to predict the Ultimate tensile strength of the laser welded Joint at 95% confidence level.
2. The model has been developed to predict the Tensile Shear Strength

Empirical Relationship (**UTS**) = {(-3002.97699) + (94.46504 x **DV**) – (438.88968 x **SOD**) + (812.51551 x **OL**) + (7.75000 x **DV** x **SOD**) – (2.25000 x **DV** x **OL**) +(30.00000x **SOD** x **OL**) –(3.76234x **DV²**)+(17.14655x **SOD²**) - (53.71513x **OL²**))

3. The predicted and actual values for tensile test are evaluated and plotted. The 3D response surface plot and contour plots are also drawn for this model. The interaction effect of MPW parameters (Discharge Voltage and Stand-off distance), (Discharge Voltage and Overlap Length) & (Stand-off distance and Overlap Length) on the Tensile Shear Strength have been plotted and discussed.
4. The optimized value for ultimate tensile strength has been identified as 303.04 MPa. The tensile strength is maximum for the Discharge Voltage of 12.6kV, Stand-off distance 1.76mm and Overlap length 7.92mm.
5. The experimental value of tensile strength 303MPa and the predicted value obtained through the empirical relationship of 303.04 MPa fall very close and hence the developed model holds good. This model can be used to predict the tensile strength for the given set of process parameters.
6. The predicted values of process parameters through RSM was validated by conduct of five test experiments. The error percentage of 3% between the predicted and actual values shows the higher accuracy of the model.
7. The most influential parameter was found to be Discharge Voltage followed by Stand- off distance and then the Overlap length.
8. The Vickers microhardness value have been determined for the base Flyer material, base Target material and the weld interface, the hardness value was the highest in the weld interface 138 HV followed by the base Flyer material 111-113 HV and base Target material 108-117 HV.
9. Microstructure analysis has been carried out using FESEM in which microstructures shows well defined wavy interface indicating typical MPW joint.

References

[1] M. Kimchi, H. Shao, W. Cheng, P. Krishnaswamy " Magnetic Pulse Welding Aluminium tubes to Steel bars" Welding in the World volume 48, pages19–22 (2004)

[2] Furth, H. P., Waniek, R. W.: "Production and use of high transient magnetic fields, part I," Rev. Sci. Instr., (1956), vol. 27, p. 195.

[3] Furth, H. P., Levine, M. A., Waniek, R. W.: "Production and use of high transient magnetic fields, part II," Rev. Sci. Instr., (1957), vol. 28, p. 949.

[4] R. M. Mirandaa, B. Tomás a, T. G. Santosa, N. Fernandes b "Magnetic pulse welding on the cutting edge of industrial applications" Soldag. Insp. São Paulo, Vol. 19, Nº. 01, p.069-081, Jan/Mar 2014 69

[5] Mishra, Shobhna, Sharma, SurenderKumar,Kumar, Satendra,Sagar, Karuna, Meena, Manraj, Shyam, Anurag "40kJ Magnetic PulseWelding System for Expansion Welding of Aluminium 6061 Tube" Journal of Materials Processing Technology http://dx.doi.org/10.1016/j.jmatprotec.2016.09.020

[6] R.N. Raoelisona, N. Buirona, M. Rachika, D. Haye b, G. Franzc, M. Habakc, "Study of the elaboration of a practical weldability window in magnetic pulse welding", Elsevier-Journal of Material Processing Technology/4 March 2013.

[7] Koen Faes, Irene Kwee and Wim De Waele," Electromagnetic Pulse Welding of Tubular Products: Influence of Process Parameters and Workpiece Geometry on the Joint Characteristics and Investigation of Suitable Support Systems", Metals- MDPI/01st May 2019.

[8] Pampa Gosh, Suman Patra, Soumya Chatterjee, Mahadev Shome "Microstructural Evaluation of Magnetic Pulse Welded Plain Carbon Steel Sheets" Journal of Materials Processing Technology/4 November 2017

[9] Haiping Yu , Zhidan Xu , Zhisong Fan, Zhixue Zhao, Chunfeng Li " Mechanical property and microstructure of aluminum alloy-steel tubes joint by Magnetic pulse welding" Elsevier-Materials Science & Engineering A/ 10 November 2012

[10] Joerg Bellmann, Joern Lueg-Althoff, Sebastian Schulze,Soeren Gies, Eckhard Beyer, and A. Erman Tekkaya "Parameter Identification for Magnetic Pulse Welding Applications" Key Engineering Materials ,ISSN: 1662-9795, Vol. 767, pp 431-438,doi:10.4028/www.scientific.net/KEM.767.431 © 2018 Trans Tech Publications, Switzerland

[11] Ben-Artzy , A. Stern, N. Frage , V. Shribman , O. Sadot " Wave formation mechanism in Magnetic Pulse Welding" International Journal of Impact Engineering 37 (2010) 397–404

[12] Yuan Zhang, Sudarsanam Suresh Babu & Glenn S. Daehn " Interfacial ultrafine-grained structures on aluminum alloy 6061 joint and copper alloy 110 joint fabricated by magnetic pulse welding" Springer, Journal of Material Science (2010) 45:4645–4651 DOI 10.1007/s10853-010-4676-0.